Optical properties of ZnO nanoparticles synthesized by varying the sodium hydroxide to zinc acetate molar ratios using a Sol–Gel process

Article *in* Central European Journal of Physics · October 2011

DOI: 10.2478/s11534-011-0050-3

Cent. Eur. J. Phys. • 9(5) • 2011 • 1321-1326
DOI: 10.2478/s11534-011-0050-3

VERSITA

Central European Journal of **Physics**

Optical properties of ZnO nanoparticles synthesized by varying the sodium hydroxide to zinc acetate molar ratios using a Sol-Gel process

Research Article

Francis B. Dejene[1]*, Abdub G. Ali[1], Hendrik C. Swart[2], Reinhardt J. Botha[3], Kittesa Roro[4], Liza Coetsee[2], Mart M. Biggs[2]

1 *Department of Physics, University of the Free State (Qwaqwa Campus), Private Bag X13, Phuthaditjhaba, 9866, South Africa*

2 *Department of Physics, University of the Free State, P.O. Box 339, Bloemfontein, 9300, South Africa*

3 *Department of Physics, Nelson Mandela Metropolitan University, P.O. Box 77000, Port Elizabeth, 6031, South Africa*

4 *Department of Physics, Physics Department, University of Pretoria, Lynnwood Road, Pretoria 0002, South Africa*

Received 24 September 2010; accepted 27 April 2011

Abstract: Material property dependence on the OH^-/Zn^{2+} molar ratio of the precursor was investigated by varying the amount of NaOH during synthesis of ZnO. It was necessary to control the water content and temperature of the mixture to ensure the reproducibility. It was observed that the structural properties, particle size, photoluminescence intensity and wavelength of maximum intensity were influenced by the molar ratio of the precursor. The XRD spectra for ZnO nanoparticles show the entire peaks corresponding to the various planes of wurtzite ZnO, indicating a single phase. UV measurements show the absorption that comes from the ZnO nanoparticles in visible region. The absorption edge of these ZnO nanoparticles are shifted to higher energies and the determined band gap energies are blue shifted as the OH^-/Zn^2 molar ration increases, due to the quantum confinement effects. The photoluminescence characterization of the ZnO nanostructures exhibited a broad emission band centred at green (600 nm) region for all molar ratios except for $OH^-/Zn^{2+} = 1.7$ where a second blue emission around 468 nm was also observed. The photoluminescence properties of ZnO nanoparticles were largely determined by the size and surface properties of the nanoparticles.

PACS (2008): 61.46.-w, 78.90.+t, 81.07.-b, 82.90.+j

Keywords: nanomaterials • semiconductor • NaOH molar ratio • ZnO: luminescence

*E-mail: dejenebf@qwa.uovs.ac.za

1. Introduction

Semiconductor nanoparticles are a very important topic in the ongoing research activity across the world [1]. The semiconductor particles exhibit size-dependant properties such as scaling of the energy gap and corresponding change in the optical properties. They are considered as the front-runners in the technologically important materials. ZnO is attracting tremendous attention due to its electronic properties. It has a wide and direct band gap of 3.37 eV at room temperature and it has a large exciton binding energy of 60 meV. As a result of its excellent chemical and physical properties [1–5], ZnO has been widely used in low-voltage phosphor material, sensors, photovoltaics, photonics, light-emitting devices, photo detectors, optical waveguides, transparent conductive films, and bulk acoustic wave devices [6–9]. ZnO as luminescent nanomaterials in the form of nanoparticles, nanorods, nanowires, nanotubes, nanocomposites as well as colloidal or bulk nanocrystals are of interest not only for basic research but also for usable applications [10–12]. High surface to volume ratio, local phenomena such as absorption or change in the surface electronic state may contribute significantly to special properties.

Many methods have been developed to prepare ZnO particles, including the sol-gel method [10], evaporative decomposition of solution [11], template-assisted growth [12], wet chemical synthesis [13], and gas-phase reaction [14]. Generally, some of the above methods require complex equipment and complicated operation, which can be called 'noble' methods. It is still a challenge to search for a simple, cheap, scalable and reproducible route to prepare metal oxides nanoparticles with a high yield and superior qualities. Herein, we report a simple sol-gel method in ethanolic solution to prepare ZnO nanoparticles. In this study the influence of the molar ratio of OH^-/Zn^{2+} on structural, morphological and optical properties of the dried pure ZnO nanoparticles were investigated.

2. Experimental

ZnO nanoparticles were prepared in an ethanol medium by the reaction of zinc acetate and sodium hydroxide. All chemicals (Aldrich make, 99.99%), used were AR grade and not further treated. The detailed preparation procedure may be summarized as follows: 0.918 g of $Zn(CH_3COO)_2$ was dissolved in 60 ml of ethanol using vigorous magnetic stirring at 80°C for 30 min followed by cooling in ice water for 5 min. To determine the dependence of the prepared ZnO nanoparticles on the NaOH content of the precursors various weights of NaOH pellets (as shown in Table 1) were dissolved in 20 ml of ethanol in an ultrasonic bath to change the pH of the solution, and cooled in ice water as well. These solutions were slowly added to the Zn^{2+} solution using vigorous stirring in ice water. Stirring ran for 24 hrs and the solution slowly gels and finally turns whitish colloidal solution. After centrifugally separated from the solutions, repeatedly washed using a mixture of ethanol and heptane with volume ratio 3:1, the obtained white precipitates were dried at ambient condition in a fume hood for 2 days. To determine the annealing and crystallization temperature of the as prepared ZnO nanoparticles, the thermal analysis was carried out with a Perkin-Elmer DSC 7 differential scanning calorimeter (DSC), and Thermo gravimetric analyses (TGA) were performed in a Perkin-Elmer TGA7 thermo gravimetric analyzer. The morphology of the ZnO powders annealed at 300°C was observed by a Shimadzu Superscan SSX-550 system scanning electron microscope (SEM) operated at 20 kV equipped with energy dispersive X-ray spectroscopy (EDS). Transmission electron microscope (TEM) image were recorded on a Philips EM420 transmission electron microscope. The X-ray diffraction (XRD) patterns were recorded to characterize the phase and crystal structure of the nanoparticles using a multi-purpose XRD system with a Siemens Diffractometer D5000 with a Cu K_α radiation source at 40 kV, 30 mA and $\lambda = 1.5418$ Å. Optical absorption was performed on an Agilent HP1100 diode-array UV-visible spectrophotometer. Room temperature photoluminescence (PL) of the samples was measured, using a He-Cd laser (325 nm) as excitation sources.

Table 1. Composition of precursors for different ZnO nanostructures.

Precursors	No. of moles of NaOH	No of Moles of $Zn(CH_3COO)^2$ $\times 10^{-3}$	OH^-/Zn^{2+} Molar ratio	PH
1	0	3.15	0	5.6
2	5.5×10^{-3}	3.15	1.7	8.1
3	8.25×10^{-3}	3.15	2.6	10.1
4	1.1×10^{-2}	3.15	3.5	11.4
5	1.375×10^{-2}	3.15	4.4	11.5
6	1.65×10^{-2}	3.15	5.2	11.4
7	1.925×10^{-2}	3.15	6.1	11.5
9	2.2×10^{-2}	3.15	7	11.4

3. Results and discussions

3.1. Thermal properties

TGA – DSC curves of as deposited ZnO nanoparticles are shown in Fig. 1. There was a total weight loss of 13 wt. %

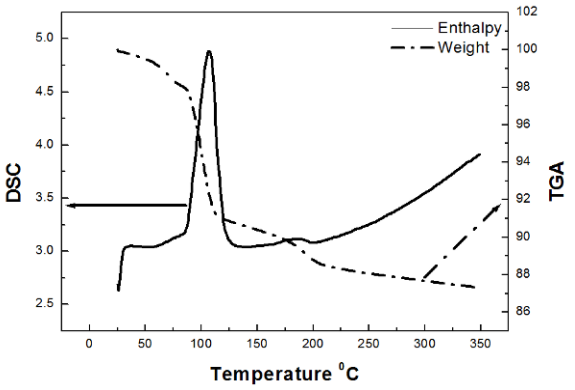

Figure 1. DSC-TGA heating curves of the ZnO nanoparticles samples from 23 to 350°C.

when the sample was heated from room temperature to 350°C. Three weight losses were observed in the temperature regions RT – 60°C, 90 – 120°C and 150 – 350°C. Weight loss of about 2 wt. % from room temperature to 60°C was due to desorption of the physically adsorbed water and partly chemically adsorbed alcohol. The weight loss of 7 wt. % from 90 to 120°C was due to the removal of chemically adsorbed water and alcohol. Weight loss of almost 3 wt. % from 120 to 350°C was mostly due to the decomposition of organic mater and the hydroxide groups. Two endothermic peaks (100°C; 192°C) were found in the heating process. The endothermic peak at 100°C in DSC results from evaporation of solvent. The broad endothermic peak around 192°C results from the decomposition of residual organics and crystallization of the ZnO. There is a slight gradual weight loss of ZnO after 250°C as observed from TGA curve. Hence the as prepared ZnO samples are annealed at 600°C for crystallization.

3.2. Morphological and structural properties

The morphology and size of the dried ZnO nanoparticles were examined by SEM observations. By adjusting the OH^-/Zn^{2+} molar ratios, many ZnO nanostructures with approximately similar morphological properties were obtained, in particular the range of the molar ratios investigated. A representative SEM image of ZnO powder dried at ambient conditions in a fume hood for 2 days is presented in Fig. 2. The presence of highly agglomerated morphology should be attributed to overlapping of smaller and medium particles. However, small agglomerates on some of the large particles are clearly visible at high magnifications. Therefore it is concluded that the chosen OH^-/Zn^{2+} molar ratio range has minimum influence on the morphology of the ZnO samples.

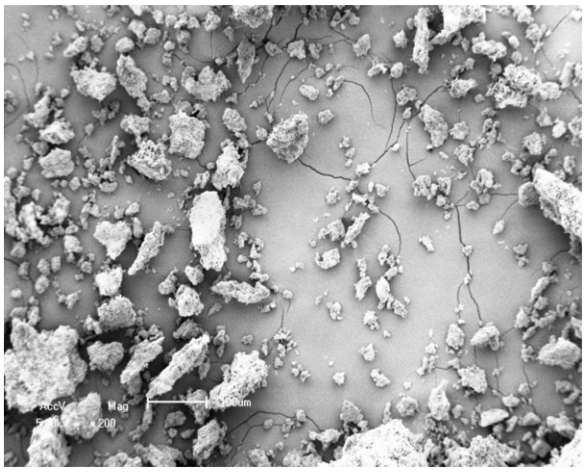

Figure 2. SEM image of agglomerated ZnO.

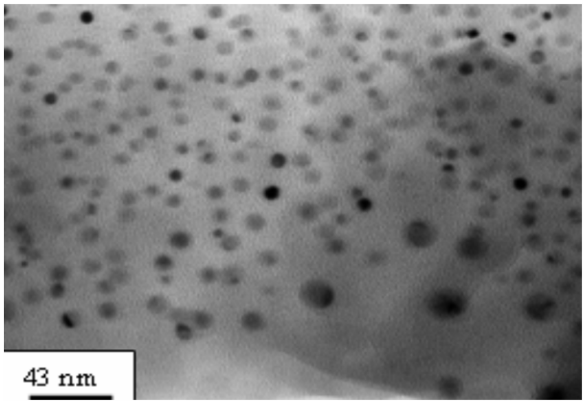

Figure 3. TEM image of dried ZnO nanoparticles.

Fig. 3 shows the TEM image of ZnO nanopowders with OH^-/Zn^{2+} molar ratio equal to 1.7. As shown in the figure the powder was monodispersed with nearly spherical nanoparticles with a mean size of between 5 – 20 nm. The presence of some bigger particles should be attributed to the aggregating or overlapping of smaller particles. The TEM observation further confirmed the calculated average size of ZnO nanoparticles with OH^-/Zn^{2+} molar ratio equal to 1.7. To determine the elemental composition of our matrices, EDS spectra were taken. For all ZnO samples which were dried for 2 days in air, all expected elements (Zn, O) were detected and the adventitious carbon is also to be seen. Fig. 4 shows the XRD pattern obtained from a typically dried ZnO powder. The results indicate that ZnO has been successfully prepared by a sol-gel process. The observed diffraction peaks are well-matched with the typical single crystalline wurtzite

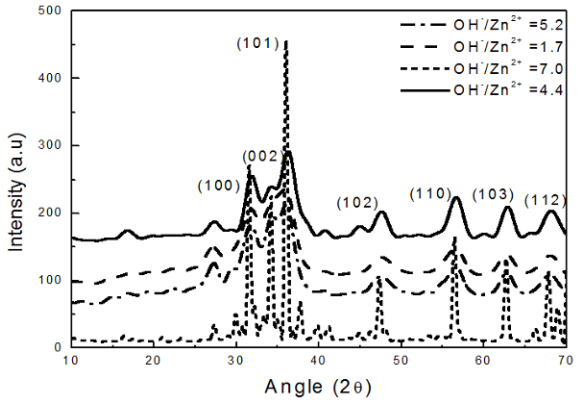

Figure 4. X-ray diffraction spectrum of the prepared ZnO nanoparticles using different molar ratio of OH^-/Zn^{2+}.

hexagonal phase bulk ZnO (JCPDS, card no. 36-1451). No other peaks of impurities such as Zn or $Zn(OH)_2$ were detected within the detection limit of the X-ray diffraction instrument. The intense peaks in the diffraction spectrum show the high-crystallinity of the dried powders. The peaks are broad due to the nanocrystalline nature of the obtained powder. The average grain size (D) of the prepared nanoparticles was calculated using Debye-Scherrer formula [15]

$$D = \frac{0.9\lambda}{\beta \cos\theta},$$

where $\lambda = 0.154$ nm is the wavelength of the X-ray radiation used, θ the Bragg diffraction angle of the XRD peak and β is the measured broadening of the diffraction peak at an angle of 2θ, at half its maximum intensity (FWHM) in radians. It is found that the average grain size reduced with molar ratio until $OH^-/Zn^{2+} = 4.4$ and increased again as the molar ratio increased. The average grain size was estimated as 10 nm for OH^-/Zn^{2+} molar ratio equal to 1.7, 9 nm for 4.4, 12 nm for 5.2 and 44 nm for 7. The results are partly in agreements with the absorption spectra examined by Sakohara et al. [16], who claimed that the crystallite size increased with the lithium hydroxide concentration for the range investigated. It is concluded that the crystallite size of the ZnO nanoparticles are dependent on the amount of NaOH added. The calculated nanoparticle sizes for ZnO sample with OH^-/Zn^{2+} molar ratio of 1.7, corresponds well to that depicted by the TEM image of the said sample. Similar results have been reported by Abdullah et al. [17] and Ntwaeaborwa and Holloway [18] from ZnO colloid prepared by hydrolysis method and sol gel synthesized ZnO nanoparticles respectively.

3.3. Optical properties

Figure 5 shows UV-Vis optical absorption spectra of the dried ZnO samples. In general absorption and transmission spectra probe the crystalline internal molecular orbital and provide information concerning size and particle compositions [18]. The absorbance decreases (band gap increases) with an increase in OH^-/Zn^{2+} molar ratio up to 8.8, but for OH^-/Zn^{2+} molar ratio of 4.4 its distinctively high. It is clearly visible from absorbance spectra that the excitonic absorption peak of ZnO nanoparticles appears around 360 nm for selected molar ratios, which lies much below the bandgap wavelength of 375 nm ($E_g = 3.3$ eV) of bulk ZnO [16], indicating that the particles must be comparable to the Bohr radius of exciton for ZnO. It is also observed that absorption edge of ZnO is very sharp for OH^-/Zn^{2+} molar ration of 0.44, 0.55 and 0.88 that indicates the monodispersed nature of the nanoparticle distribution [19]. The monodispresed nature of particle distribution for OH^-/Zn^{2+} molar ration of 1.7 have also been confirmed by TEM measurement as shown in Fig. 3. The relatively high absorbance at longer wavelengths and broad absorption edge for OH^-/Zn^{2+} molar ration of 0.22 indicates large dispersion in size of the ZnO nanostructures and their arbitrary orientations. Combination of low visible absorbance displayed by the ZnO nanoparticles and low electrical resistivity is very useful in applications such as transparent electrodes in solar cells, luminescence display screens and ultraviolet diodes [16]. Insert in Fig. 6 depicts plot of α^2 versus $h\nu$ for deposited ZnO nanoparticles. The extrapolation of the linear portion of $(\alpha h\nu)^2$ versus $h\nu$ graph at $\alpha = 0$ yields the band gap value of the nanoparticles [20, 21]. The band gap of prepared ZnO around 3.3 eV agrees well with the values generally re-

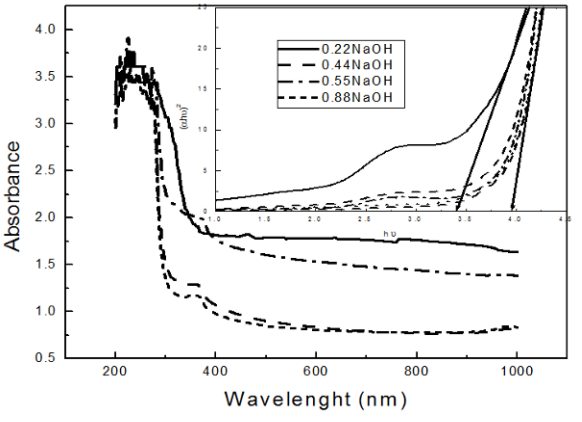

Figure 5. UV-VIS absorption characteristics of ZnO nanoparticles dispersed in distilled water. Inset shows the $(\alpha h\upsilon)^2$ vs $h\upsilon$ graph.

ported in literature [16]. It can also be seen from Fig. 6 that band gap value slightly increases to approximately 4.0 eV with an increase in OH^-/Zn^{2+} molar ratio except for molar ratio of 4.4 where the band gap doesn't seem to obey the proportionality relationship.

Fig. 6a shows the PL emission spectra for the ZnO powder excited with a He-Cd laser (325 nm). Clearly, two bands were observed from the room-temperature PL spectrum of the ZnO nanoparticles for molar ratio of 1.7 i.e., blue emission and green-yellow emission at 468 and around 580 nm, respectively. Interestingly, it was observed that, the green emission is enhanced while blue luminescences is quenched and completely disappear in most cases with variation in molar ration. The results confirm broad luminescence in the green-yellow region [18] for ZnO powder. The green emission is also known to be a deep level emission which is caused by the impurities and structural defects in the crystal such as oxygen vacancies, zinc interstitials, etc. Vanheusden et al. [22] proposed the mechanism of green emission and reported that green emission is due to the recombination of the electrons in singly occupied oxygen vacancies in ZnO and that the emission results due to the recombination of a photo-generated hole with an electron occupying the oxygen vacancies. It is also reported that particles surface depletion plays a major role in the density of singly ionized oxygen vacancies and the charge state of this defect and thus is controlling the green emission intensity [23, 24].

Regarding the appearance of blue emission in ZnO nanomaterials, Dai et al. reported that blue emission at 460 nm might be due to intrinsic defects such as oxygen and zinc interstitials [22]. However, the exact mechanism behind this emission is still unclear.

As shown in Fig. 6b, the intensity of the broad green PL peak and the corresponding emission peak position were also affected by the OH^-/Zn^{2+} molar ratios in the precursor solution. As the OH^-/Zn^{2+} molar ratio increases to about 5.5, the green luminescence intensity increases to a maximum value and then reduces thereafter. On the contrary the relative peak positions of green emission portray on average a linear relationship with concentration of NaOH. Fig. 6c shows that the emission wavelength (energy) has an exponential increase with the grain size. The increases in emission energy are attributed to the particle size variation of the dried ZnO nanoparticles as the molar ratios of $OH-/Zn^{2+}$ vary. The decreases in particles size increase the band gap energy; correspond to larger transition energy from the valence band to the location of delocalized electrons at singly occupied oxygen vacancies within deep trapped holes. It was observed therefore that not only does the molar ratio of OH^-/Zn^{2+} of the precursor influence the size of the prepared nanoparticles, but

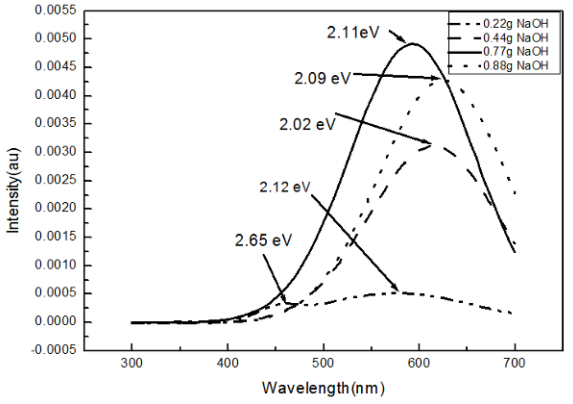

a

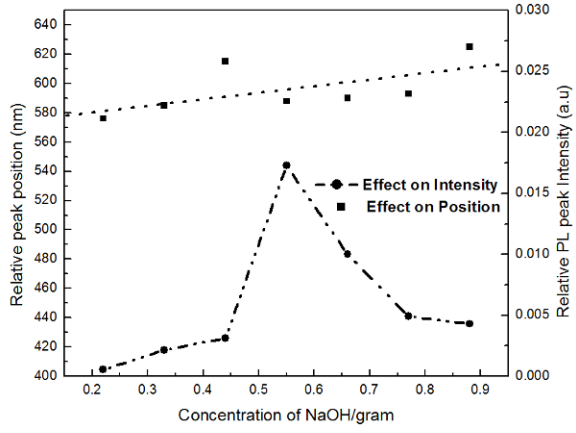

b

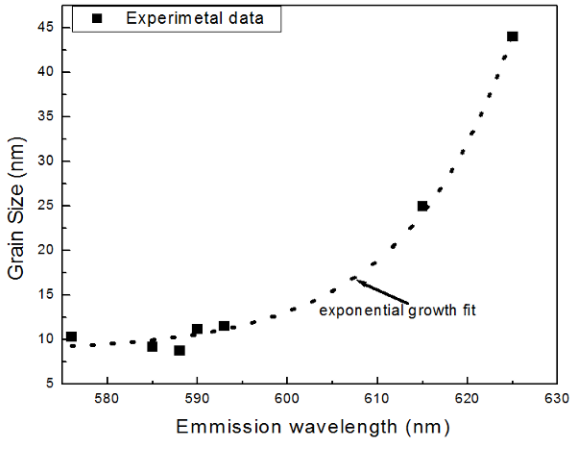

c

Figure 6. (a) PL emission spectra of ZnO nanoparticles prepared by various concentration of NaOH in the precursor. (b) Effect of NaOH concentration on the intensity of the broad PL peaks and corresponding emission wavelength. (c) The dependence of emission wavelength (energy) on the NaOH concentration.

also significantly control the emission energy and maximum luminescence intensity.
This suggests they originate from different sites in the ZnO phosphor. The visible luminescence in ZnO has been proposed to be caused by the breakage of excitons where by an electron decays non-radiatively to the defect states in the optical gap and then radiatively recombining with the holes at the valency band. In nano-crystalline ZnO, due to increase in the surface area/volume ratio, the luminescence from the defect states is large. For device application therefore such defect states should be controlled to reduce the visible deep level emission.

4. Conclusion

In summary, high quality luminescent ZnO powder with different sizes was prepared by wet chemical synthesis through a sol gel process just by adjusting the molar ratio of sodium hydroxide to zinc acetate. XRD confirmed the wurtzite structure of ZnO. All elements expected in the nanoparticles were observed through EDX. SEM showed agglomerated particles albeit with nanosized agglomerates on the surface and which were interpreted as the building particles of the bigger ones. A further indication to nanosized particles of the ZnO powder was revealed by the TEM image, increase in band gap and blue shifted luminescence of both UV-vis and PL measurements. The deep level defect emission luminescence is predominant for the prepared ZnO nanoparticles by sol-gel, while the intensity of the green emission luminescence is optimum for OH^-/Zn^+ molar ratio of 4.4. This enhanced luminescence was attributed to quantum confinement caused by the nano sized ZnO nanoparticles. The choice of appropriate molar ratio of the precursor is paramount in the size control of ZnO nanoparticles as no catalyst is employed.

Acknowledgment

The authors would like to acknowledge the national Research Foundation and the University of the Free State for financial support. Prof. P.W.J. van Wyk from the Centre of Microscopy (UFS) for doing SEM, BSE and EDS measurements. Also Prof. J.R. Botha, South African Research Chairs Initiative of the Department of Science and Technology and National Research Foundation for PL measurements. One of the authors (F.B. Dejene) who is a regular associate undertook part of this work with the support of the "ICTP Programme for Training and Research in Italian Laboratories, Trieste, Italy".

References

[1] J. Joo, S.G. Kwon, J.H. Yu, T. Hyeon, Adv. Mater. 15, 1873 (2005)
[2] U. Pal, P. Santiago, J. Phys. Chem. B 109, 15317 (2005)
[3] L. Vayssieres, Adv. Mater. 15, 464 (2003)
[4] L. Vayssieres, K. Keis, A. Hagfeldt, S.E. Lindquist, Chem. Mater. 13, 4395 (2001)
[5] G. Marci et al., J. Phys. Chem. B 105, 1026 (2001)
[6] Z.K. Tang et al., Appl. Phys. Lett. 72, 3270 (1998)
[7] S. Shionoya, W.M. Yen, Phosphor Handbook (CRC Press, Boca Raton, FL, 1999) 255
[8] B. O'Regan, M. Gratzel, Nature 353, 737 (1991)
[9] A.V. Dijken, E.A. Mulenkamp, D. Vanmaekelbergh, A. Meijerink, J. Lumin. 90, 123 (2000)
[10] C. Feldmann, T. Justell, C.R. Ronda, P.J. Schmidt, Adv. Funct. Mater. 13, 101 (2003)
[11] A.S. Edelstein, R.C. Cammarata, Nanomaterials: Synthesis, Properties and Applications (Institute of Physics Publishing, Bristol, Philadelphia, 1996)
[12] B.R. Ratna et al., The 5th International Conference on the Science and Technology of Display Phosphors, 8-10 November 1999, San Diego, California, USA, 295
[13] H. Weller, Adv. Mater. 5, 88 (1993)
[14] R.J. Lanf, W.D. Bond, Am. Ceram. Soc. Bull. 63, 278 (1984)
[15] H.R. Fallah, M. Ghasemi, A. Hassanzadeh, H. Steki, Physica B 373, 274 (2006)
[16] S. Sakohara, M. Ishida, M.A. Anderson, J. Phys. Chem. B 102, 10169 (1998)
[17] M. Abdulah, T. Morimoto, K. Okuyama, Adv. Funct. Mater. 13, 1 (2003)
[18] O.M. Ntwaeaborwa, P.H. Holloway, Nanotechnology 16, 865 (2005)
[19] S.M. Haile, D.W. Johnson, G.H. Wiseman, J. Am. Ceram. Soc. 72, 2004 (1989)
[20] L.E. Brus, Nanostruct. Matter. 1, 71 (1992)
[21] L.E. Brus, J. Chem. Phys. 79, 5566 (1983)
[22] Z. Zhang et al., J. Phys. Chem. B 110, 8566 (2006)
[23] Y. Ni et al., Nanotechnology 18, 155603 (2007)
[24] G.E. Malashkevich, I.M. Melichenko, E.N. Poddenezhny et al., J. Non-Cryst. Solids 260, 141 (1999)